Journal of the Korean Nuclear Society
Volume 28, Number 4, pp. 405~415, August 1996

Numerical Analysis for Unsteady Thermal Stratified Turbulent Flow in a Horizontal Circular Cylinder

Jang-Sun Ahn, Yong-Sang Ko, and Byeong-Ho Park
Korea Atomic Energy Research Institute
150 Dukjin-dong, Yusong-gu, Taejon 305-353, Korea

Hag-Ki Youm and Man-Heung Park
Korea Power Engineering Company, Inc.
369-9. Mabok-ri, Kusung-myon, Yongin-gun, Kyunggi-do, Korea

(Received March 21, 1996)

Abstract

In this paper, the unsteady 2-dimensional turbulent flow model for thermal stratification in a pressurizer surge line of PWR plant is proposed to numerically investigate the heat transfer and flow characteristics. The turbulence model is adapted to the low Reynolds number K-ε model (Davidson model). The dimensionless governing equations are solved by using the SIMPLE (Semi-Implicit Method for Pressure Linked Equations) algorithm. The results are compared with simulated experimental results of TEMR Test. The time-dependent temperature profiles in the fluid and pipe wall are shown with the thermal stratification occurring in the horizontal section of the pipe. The corresponding thermal stresses are also presented. The numerical result for thermal stratification by the outsurge during heatup operation of PWR shows that the maximum dimensionless temperature difference is about 0.83 between hot and cold sections of pipe wall and the maximum thermal stress is calculated about 322MPa at the dimensionless time 28. 5 under given conditions.

1. Introduction

Thermal stratification and striping phenomena are reported to occur in the piping system of nuclear power plants. These phenomena are usually observed in the pipe line of the safety related systems and may be identified as the source of fatigue damage in the piping system due to the thermal stress loadings which are associated with plant operation modes.

The typical thermal stratification can occur in the horizontal section of the surge line during insurge or outsurge. In addition, the temperature changes in the fluid region due to the thermal stratification bring about an axial and a circumferential stress in the pipe.

The thermal stratification is accompanied with the fluctuation of interface level which is referred to as thermal striping. The thermal striping also produces a local thermal stress in the pipe [9,15]. Since the thermal striping amplitude is usually very small, it is assumed that this layer is not considered in the analysis.

The propensity for a stratification of fluid in the horizontal pipe can be correlated to Richardson num

ber (Ri) which is the ratio of the gravitational force to inertial force acting on the fluid. If this number is greater than unity, the thermal stratification can be expected to occur. The buoyant force is caused by the density difference between the hot and cold fluid and its magnitude is related to the temperature difference. Therefore, the thermal stratification is likely to occur when the flow velocity is low and the temperature difference is large.

This phenomenon of thermal stratification plays an important role in the piping integrity, because the significant thermal stresses are induced by the failure and the unexpected motions in piping lines of PWR [12,13]. Since then, the thermal stresses due to the stratification of the hot and cold fluids have been considered by the utilities and vendors for the design and licensing processes of the piping [5,9,14]. As a result, these pipes of the PWR have been recently designed using the results of simple analyses, experiments or monitoring [4,8,15,17].

Since Fraikin et al [7] applied the K-ε model proposed by Launder and Spalding [10] to analyze the turbulent buoyance force problem in an enclosure, some investigations on turbulent buoyance force in an enclosed space have been carried out. For a horizontal circular cylinder, Farouk [6] employed the K-ε model to obtain numerical solution of the turbulent natural convection. He had question about the use of wall function to analyze the turbulent flow by buoyance in enclosure. Viollet [16] studied the experiment and numerical modelling of the density effects following a change in the inlet temperature using the unsteady K-ε model for turbulence. Davidson [3] applied the modified form of a low Reynolds number K-ε turbulence model to analyze the turbulent natural convection problem in a tall rectangular cavity of 5 : 1 aspect ratio.

The potential for the thermal stratification is the greatest during heatup and cooldown conditions because of the largest temperature difference between the pres- surizer and hot leg of PWR [12,14].

Based on this fact, in this study, the phenomena of unsteady thermal stratified turbulent flow in a horizontal circular cylinder have been investigated numerically with the low Reynolds number K-ε turbulent model (Davidson model [3]) when the thermal stratification in the horizontal pipe of a pressurizer surge line occurred by outsurge during heat-up operation of PWR.

2. Model Formulation

At normal operation, since the difference of temperature between the pressurizer and the hot leg is relatively small, the effects of thermal stratification has been observed to be small. However, during the some modes of plant heatup and cooldown, the temperature difference in system could be as high as 167℃, in which the effects of the thermal stratification must be accounted for. The potential for thermal stratification is increased as the difference of tem perature between the pressurizer and the hot leg increases and as the surge flow rates decrease. Therefore, in this study, the heatup mode is selected for analysis model as shown in Fig. 1 (a). Symmetry allows half of the pipe cross section to be considered as shown in Fig. 1(b).

The major assumptions to solve the governing equations are as follows;

(a) the flow of hot and cold fluids is 2-dimensional,
(b) the thermal and hydrodynamic conditions are symmetrical with respect to the vertical center line,
(c) the properties of fluid and solid except density in the body force term are treated as constant,
(d) the compressibility effects, viscous dissipation and radiation heat transfer of fluids are neglected,
(e) the thickness of the interface layer is neglected, and
(f) the interface level is changed only from top to center of the piping during the constant time when the hot fluid with constant low velocity flows into a upper region of the stagnant cold

fluid.

A linear variation of density with temperature is assumed according to the following equation

$$\rho = \rho_f \{1 - \beta (T^* - T^*_{atm})\} \quad (1)$$

Some simplification of the resulting body force terms is represented by defining an effective pressure,

$$P^* = P' + \rho_f g r^* \cos\theta \quad (2)$$

Dimensionless variables are formed as follows :

$$r = \frac{r^*}{r_i^*},\ a = \frac{r_o^* - r_i^*}{r_i^*},\ u = \frac{u^*}{U_o},\ v = \frac{v^*}{U_o},\ t = \frac{t^* U_o}{r_i^*},$$

$$K = \frac{k^*}{U_o^2},\quad \varepsilon = \frac{\varepsilon^* r_i^*}{U_o^3},\quad P = \frac{P^*}{\rho_f U_o^2},$$

$$T = \frac{T^* - T^*_{cold}}{T^*_{hot} - T^*_{cold}},\quad \mu_t = \frac{\mu_t^*}{\mu},\quad \mathrm{Pr} = \frac{C_p \mu}{k_f}, \quad (3)$$

$$Re = \frac{U_o r_i^*}{\nu},\quad Gr = \frac{g \beta r_i^{*3} (T^*_{hot} - T^*_{cold})}{\nu^2},$$

$$Bi = \frac{h (r_o^* - r_i^*)}{k_s}$$

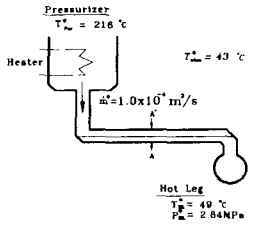

(a) The Heatup Condition

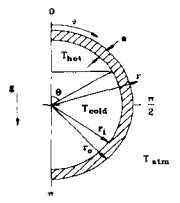

(b) Schematic Diagram of Calculation Domain (A'-A)

Fig. 1. The Heatup Condition and Calculation Domain of the Surge Line

where, Uo is the constant velocity in the axial direction and asterisks represent the dimensional values. Although the fluid flow is assumed to be two dimensional, the axial velocity is used to define the dimensionless parameter, Ri ($=Gr/Re^2$).

For a unsteady two-dimensional flow, the following governing equations represent the conservation of the dimensionless time-averaged quantities. The same 2-D low Reynolds number K-ε model for turbulence as employed by Davidson [3] has been used for the present study.

$$\frac{1}{r}\frac{\partial}{\partial r}(rv) + \frac{1}{r}\frac{\partial}{\partial\theta}(u) = 0$$

$$\frac{\partial u}{\partial t} + \frac{1}{r}\frac{\partial}{\partial r}(ruv) + \frac{1}{r}\frac{\partial}{\partial\theta}(u^2) = -\frac{1}{r}\frac{\partial P}{\partial\theta} + D_1\left\{\frac{1}{r}\frac{\partial}{\partial r}\left(r\frac{\partial u}{\partial r}\right) + \frac{1}{r}\frac{\partial}{\partial\theta}\left(\frac{1}{r}\frac{\partial u}{\partial\theta}\right)\right\} + S_u \quad (5)$$

$$\frac{\partial v}{\partial t} + \frac{1}{r}\frac{\partial}{\partial r}(rv^2) + \frac{1}{r}\frac{\partial}{\partial\theta}(uv) = -\frac{\partial P}{\partial r} + D_1\left\{\frac{1}{r}\frac{\partial}{\partial r}\left(r\frac{\partial v}{\partial r}\right) + \frac{1}{r}\frac{\partial}{\partial\theta}\left(\frac{1}{r}\frac{\partial v}{\partial\theta}\right)\right\} + S_v \quad (6)$$

$$\frac{\partial\phi}{\partial t} + \frac{1}{r}\frac{\partial}{\partial r}(rv\phi) + \frac{1}{r}\frac{\partial}{\partial\theta}(u\phi) = D_2\left\{\frac{1}{r}\frac{\partial}{\partial r}\left(r\frac{\partial\phi}{\partial r}\right) + \frac{1}{r}\frac{\partial}{\partial\theta}\left(\frac{1}{r}\frac{\partial\phi}{\partial\theta}\right)\right\} + S_\phi \quad (7)$$

where D_1 and D_2 in the equation (5), (6) and (7) represent the diffusion coefficients in the momentum equations and the other equations such as energy, kinetic energy and rate of dissipation of turbulent energy equation, respectively, which state

$$D_1 = \begin{cases} \dfrac{1}{Re}(1+\mu_t) & \textit{at fluid} \\ \infty & \textit{at solid} \end{cases} \quad (8a)$$

$$D_2 = \begin{cases} \dfrac{1}{Re}\left(\dfrac{1}{\mathrm{Pr}} + \Gamma_\phi\right) & \textit{at fluid} \\ \dfrac{\alpha_s/\alpha_f}{Re \cdot \mathrm{Pr}} & \textit{at solid (energy equation)} \\ \infty & \textit{at solid } (K \text{ and } \varepsilon \textit{ equation}) \end{cases} \quad (8b)$$

where Γ_ϕ is the exchange coefficient for the transport of property ϕ ($=$T, K and ε).

$$\Gamma_T = \frac{\mu_t}{\sigma_T} \quad \text{at energy equation} \tag{9a}$$

$$\Gamma_K = \frac{\mu_t}{\sigma_K} \quad \text{at } K \text{ equation} \tag{9b}$$

$$\Gamma_\varepsilon = \frac{\mu_t}{\sigma_\varepsilon} \quad \text{at } \varepsilon \text{ equation} \tag{9c}$$

The source term, S, in the governing equations are as follows;

$$S_u = \frac{1}{Re}\left\{\frac{1}{r}\frac{\partial}{\partial\theta}\left(\mu_t\left(\frac{1}{r}\frac{\partial u}{\partial\theta}+\frac{2v}{r}\right)\right) + \frac{1}{r}\frac{\partial}{\partial\theta}\left(\mu_t\cdot r\left(\frac{1}{r}\frac{\partial v}{\partial\theta}-\frac{u}{r}\right)\right) + \frac{\mu_t}{r}\left(\frac{\partial u}{\partial r}+\frac{1}{r}\frac{\partial v}{\partial\theta}-\frac{u}{r}\right)\right\} - \frac{uv}{r} - \frac{2}{3}\frac{1}{r}\frac{\partial K}{\partial\theta} - \frac{Gr}{Re^2}\cdot T\cdot\sin\theta \tag{10a}$$

$$S_v = \frac{1}{Re}\left\{\frac{1}{r}\frac{\partial}{\partial\theta}\left(\mu_t\cdot r\frac{\partial}{\partial r}\left(\frac{u}{r}\right)\right)+\frac{1}{r}\frac{\partial}{\partial r}\left(\mu_t\cdot r\frac{\partial v}{\partial r}\right) - \frac{2\mu_t}{r^2}\frac{\partial u}{\partial\theta} - \frac{2\mu_t}{r^2}v\right\} + \frac{u^2}{r} - \frac{2}{3}\frac{\partial K}{\partial r} + \frac{Gr}{Re^2}\cdot T\cdot\cos\theta \tag{10b}$$

$$S_T = 0 \tag{10c}$$

$$S_K = \frac{1}{Re}G - \varepsilon - B \tag{10d}$$

$$S_\varepsilon = \frac{\varepsilon}{K}\left(\frac{1}{Re}\cdot f_1\cdot C_1 G - f_2 C_2\varepsilon - C_3 B\right) \tag{10e}$$

$$G = \mu_t\left\{2\left(\frac{\partial v}{\partial r}\right)^2+2\left(\frac{1}{r}\frac{\partial u}{\partial\theta}+\frac{v}{r}\right)^2 + \left(\frac{1}{r}\frac{\partial v}{\partial\theta}+r\frac{\partial}{\partial r}\left(\frac{u}{r}\right)\right)^2\right\} \tag{10f}$$

$$B = \frac{Gr}{Re^3}\frac{\mu_t}{\sigma_T}\left(\frac{\partial T}{\partial r}\cos\theta - \frac{1}{r}\frac{\partial T}{\partial\theta}\sin\theta\right) \tag{10g}$$

The turbulent viscosity, μ_t, is related to K and ε as follows:

$$\mu_t = Re\cdot\frac{f_u\cdot C_\mu\cdot K^2}{\varepsilon} \tag{11}$$

Numerical values for C_μ, C_1, C_2, C_3, σ_T, σ_K and σ_ε are taken as recommended by Davidson[3]. They are given in Table 1.

Also, the function of f_μ, f_1 are taken as recommended by Davidson [3].

Table 1. The constant used in turbulence modeling

C_μ	C_1	C_2	C_3	σ_T	σ_K	σ_ε
0.09	1.44	1.92	1.44	0.9	1.0	1.3

$$f_u = \exp\left(-\frac{3.4}{(1+Re_t/50)^2}\right) \tag{12a}$$

$$f_1 = 1+\left(\frac{0.14}{f_u}\right)^3 \tag{12b}$$

$$f_2 = (1-0.27\exp(-Re_t^2))\,(1-\exp(-Re_n)) \tag{12c}$$

where Re_t and Re_n represent the local Reynolds number.

$$Re_t = \frac{\rho_f K^{*2}}{\mu\,\varepsilon^*} = Re\cdot\frac{K^2}{\varepsilon} \tag{13a}$$

$$Re_n = \frac{\rho_f\sqrt{K^*}n^*}{\mu} = Re\cdot\sqrt{K}\cdot n \tag{13b}$$

where n^* is the normal distance from the nearest wall. The initial and boundary conditions are as follows;

(a) $t = 0$

$0 \le r \le 1+a$: $u = v = T = 0$

$0 \le r < 1$: $K = 0.005$

$\varepsilon = 0.1\,K^2$

$1 \le r < 1+a$: $K = \varepsilon = 0$ (14a)

(b) $t > 0$

$0 \le r \le 1+a$, $\theta = 0$ and π :

$$u = \frac{\partial v}{\partial\theta} = \frac{\partial T}{\partial\theta} = \frac{\partial K}{\partial\theta} = \frac{\partial\varepsilon}{\partial\theta} = 0$$

$0 \le \theta \le \pi$ and $1 \le r \le 1+a$:

$u = v = K = \varepsilon = 0$

$0 \le \theta \le \pi$ and

$$r = 1+a : \frac{\partial T}{\partial r} = -\frac{Bi\,(T_o - T_{atm})}{a}$$

$$r = 1 : k_f\frac{\partial T_f}{\partial r} = k_s\frac{\partial T_s}{\partial r} \tag{14b}$$

3. Numerical Method and Model Verification

The governing equations have been solved by the finite volume calculation procedure including SIMPLE(Semi-Implicit Method for Pressure Linked Equations) algorithm, the power law scheme and line-by-line TDMA (Tri-Diagonal Matrix Algorithm) [13].

The preliminary tests for the number of grid system and the time step, t, have been carried out and then an optimal grid system ($r \times \theta = 62 \times 52$) and an optimal dimensionless time step, 0.003, are determined for this model.

A grid distribution in the θ-direction is decreased in accordance with the increase of the angle and the r-direction is divided into three regions. Each of the regions is uniformly arranged, but we give dense nodes near interface of fluid and pipe wall. The dimensionless time step, t, is 0.003 for the first dimensionless time 50 and after that time, increased to 0.015 to reduce the calculation time.

In order to improve convergence, the under relaxation factors of velocity, pressure, temperature, K and ε are applied 0.15, 0.45, 0.45, 0.15 and 0.15, respectively.

The converged solutions are obtained when the error of energy balance is less than 0.01% and the errors of each variables were as follows ;

$$\left| \frac{\phi^{m+1} - \phi^{m}}{\phi^{m}} \right| < 10^{-3} \qquad (15)$$

The analysis results are compared with the measured values of a TEMR (T33. 19) Test [17] to verify the program. The TEMR-experiments were to performed examine the thermal stratification behavior in a horizontal pipe. The horizontal pipe (normal diameter : 400mm, length : 6135mm) is connected to the vessel. A vertical pipe section (normal diameter : 450mm) connects to the cold fluid supply. The cold fluid enters the horizontal pipe via the elbow. The experiment conditions of TEMR-test (T33. 19) are given in Table 2.

Table 2. The condition of TEMR-experiment [17]

Simulation		PWR condition (T33.19)
Test Duration		100 sec
Average Temperature	Hot	210 ℃
	Cold	60.5 ℃
Volumetric Flow		13.003×10^{-3} m^3/sec
Cold Layer Hight		183 mm
Velocity (Cold)		24.70 cm/sec

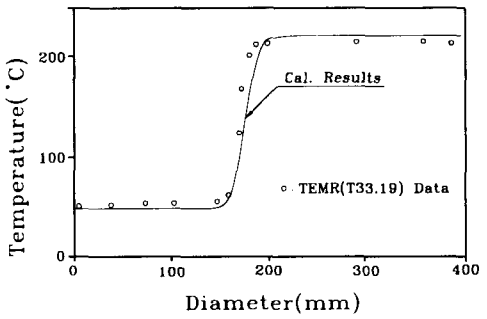

Fig. 2. The Comparison between Our Results and the TEMR Experiment (17)

The general agreement between this analysis and measured values is good except for small discrepancies near the interface.

These discrepancies are probably due to the following facts ; (a) analysis model dose not include the interface fluctuation, (b) the thermal mixing between the hot and cold fluids is not considered during the insurge time of hot fluid to the pipe line.

4. Results and Discusion

4.1 Problem Descripion

Before plant heatup, reactor coolant loops and pressurizer are filled completely. During plant heatup, heaters are on and the reactor coolant system is operated to assist in venting operations. For this time interval, the reactor coolant system is pressurized to 2.84 MPa and heated to 49 ℃. However the pressur-

izer is heated to 216 ℃ and pressurized above the 84 MPa. Therefore, the coolant in pressurizer is flowed through the surge line to the reactor coolant loops and the thermal stratification occurs in the horizontal section of surge line as Fig. 1 (a). And, considering the volume of surge line and the volume flow rate of outsurge, the calculated duration that interface level reaches from $=0$ to the $=\pi/2$ (Fig. 1 (b)) is a dimensionless time 8.58 under the given conditions and assumptions.

The design specification of surge line for the numerical analysis is shown in the Table 3 [1,2], in which the heat transfer coefficient is for the insulated pipe. All properties are calculated by the harmonic mean temperature of cold and hot fluid.

Under the above condition, the dimensionless variables are $Gr=1.9\times10^{10}$, $Re=1.52\times10^{3}$, $Pr=2.2303$ and $Bi=1.57\times10^{-3}$, and the other variables are $T_{atm}=-3.6\times10^{-2}$, $a=0.222$, $\alpha_s/\alpha_f=25.3$ and $k_s/k_f=23.6$. In this study, the numerical analysis was carried out for the above conditions.

4.2 Distribution of Flow and Temperature

Fig. 3 (a), (b), and (c) show the distribution of streamlines and isotherms at dimensionless time 3.0, 6.0 and 8.58, respectively. When by the outsurge at heatup the hot fluid with low velocity flows into a stagnant cold fluid, the interface level varies with time from $\theta=0$ to $\theta=\pi/2$ and maintains constant level on and after dimensionless time 8.58. The bracket in the Fig. 3 denotes [maximum value (interval) minimum value] of isothermal distribution.

Table 3. Design spec. of pressurizer surge line

Properties & spec.	Value
I.D of pipe	0.27 m
Thickness of pipe	0.03 m
Material of pipe	SA-312-TP-347
Conductivity	15.8 W/m℃
Heat transfer coef.	0.79 W/m^2℃
Ambient temp.	43.0 ℃

These isotherms are concentrated in a near region of interface layer, because the hot fluid flows slow in the stagnant cold fluid until dimensionless time 8.58 and the heat transfer between two fluids occurs very large. At these time, so far, the temperature of the lower section of pipe walls corresponds to temperature of cold fluid. And because of the heat transfer between hot fluid and the pipe wall, the temperature difference between inner and outer wall of pipe only occurs in the upper section of the pipe wall. Also, the potential of streamlines in the hot region are greater than those of cold region, since the hot fluid flows in the pipe until dimensionless time 8.58.

At dimensionless time 18.0, 28.5, and 60.0, the distributions of streamlines and isotherms are shown in Fig. 3 (d), (e), and (f). The profile of isotherms near of interface layer leads to change a typical temperature distribution of thermal stratification, because the heat conduction actively occurs in the pipe. As a result, the temperature difference between the inner and outer surfaces of the pipe decreases, and the distribution of flow become stable.

At dimensionless time 120.0, 240.0 and 480.0, the

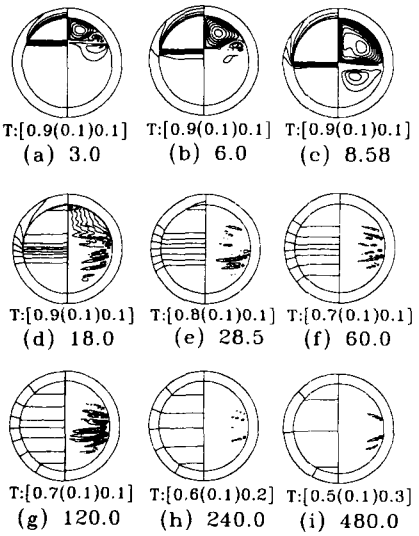

Fig. 3. The Distribution of Isotherms (left) and Streamlines (right) with Time

distribution of streamlines and isotherms are shown in Fig. 3(g), (h), and (i). Corresponding to the conduction and the natural convection in the pipe, the temperature difference between two fluids is small, and the streamline is more stabilize.

Fig. 4 shows the temperature difference ($\Delta T = T_{max} - T_{min}$) in the fluid, the inner wall and the outer wall between $\theta = 0$ and π with time, respectively. The dimensionless temperature difference of the pipe walls rapidly increase until about dimensionless time 30, but then slowly decrease after this time. On the other hand, the dimensionless temperature difference of the fluid rapidly decrease until this time. After about dimensionless time 45, the temperature difference at each regions decrease with nearly the same value. The maximum dimensionless temperature difference of the inner wall and outer wall are computed about 0.83 at dimensionless time 28.5 and about 0.80 at dimensionless time 39.0 under the given conditions, respectively. The dimensionless temperature of inner wall is somewhat greater than that of outer wall. Therefore, the maximum thermal stress by thermal stratification can be predicted along the inner wall at dimensionless time 28.5.

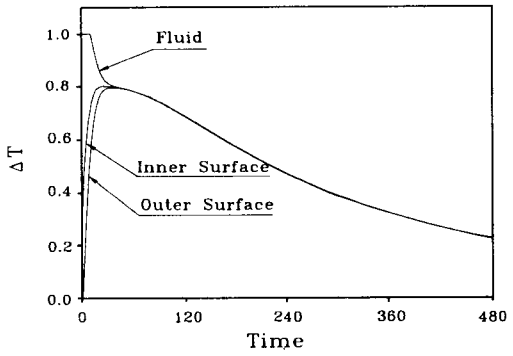

Fig. 4. The Temperature Difference of Fluid and Pipe wall

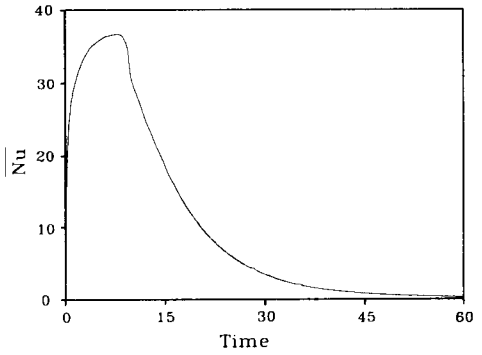

Fig. 5. The Mean Nusselt Number with Time

4.3 Heat Transfer

To analyze the heat transfer, the mean Nusselt number along the inner surface of pipe, $\overline{Nu}$ are defined

$$\overline{Nu} = \frac{\bar{h} r_i^*}{k_f} = \frac{1}{\pi} \int_0^{\pi} \left[\frac{dT}{dr} \Big|_{r=r_i} \right] d\theta \quad (16)$$

Fig. 5 shows the mean Nusselt number with time. Until dimensionless time 7.5, the mean heat transfer rate rapidly increases since temperature difference between fluid and inner wall of pipe is large. However, during dimensionless time 7.5~39.0, the decrease of the temperature difference between fluid and inner wall of pipe lead to rapidly decrease $\overline{Nu}$. After dimensionless time 39.0, it has been calculated to be almost constant. After this time, as quasi-steady state, the mean Nusselt number by the thermal mixture between two fluids is very small and heat transfer in the pipe is mostly accomplished by heat conduction.

4.4 Turbulent Quantities

Based on the turbulence modeling, the calculated turbulent quantities (K, ε and μ_t) are very small. Spec ially, the turbulent viscosity is similar to a molecular viscosity during the hot fluid level varying from top to mid-level of inner pipe. After this time, the turbulent viscosity is decreased. Also, the behavior of K and ε are similar to that of turbulent viscosity.

Even if dimensionless number (Gr) that is defined by geometrical shape and flow conditions is within a

range of turbulence region, it is not in existence the turbulent quantities because the fluid flow exist only while the hot fluid level varies from top to mid-level of inner pipe. For this duration, the heat transfer of inner pipe is mostly accomplished by heat conduction not natural convection because of the thermal stratification even if fluid temperature difference is large between the hot and cold fluid.

4.5 Thermal Stresses

Because the TEMR Tests[17] result in that the measured circumferential stresses due to the thermal stratification are small compared to the axial ones, only axial stresses are considered. In case of an infinitesimal mixing layer height and small wall thickness, the axial stresses are independent of the diameter and the thickness of the pipe. Therefore, the thermal stresses due to the thermal stratification evaluated using the simple calculation method [15] as follow;

When the pipe cannot bend, the membrane stresses in the cold ($\Theta > \theta$) and ($\Theta < \theta$) regions of a cross section can be calculated by the following equations.

$$\sigma_h = \left(\frac{\Theta}{180^0}\right) \beta \Delta T E \tag{17}$$

$$\sigma_c = -\left(1 - \frac{\Theta}{180^0}\right) \beta \Delta T E \tag{18}$$

And, in case of flexible supports, an additional linear bending stresses due to the thermal stratification are given as following equation.

$$\sigma_b = 2 \sin \frac{\Theta}{\pi} \beta \Delta T E \cos \theta \tag{19}$$

Under given conditions and assumptions, at the dimensionless time 28.5, the maximum thermal stresses that are the sum of the membrane and bending stresses are each calculated about 322 MPa at the top and the bottom of pipe inner surfaces.

This phenomenon of thermal stratification plays an important role in the piping integrity, because the significant thermal stresses are induced by the failure and the unexpected motions in piping lines of PWR. As a result, these pipes of the PWR have to design using the results of thermal stress as well as the mechanical stresses.

5. Conclusion

The unsteady phenomena of thermal stratification by the oursurge during heatup operation of PWR have been numerically investigated in horizontal surge line pipe which connects the pressurizer with the hot leg of reactor coolant system. From this study, we obtain the following conclusions.

1. Complex flow in the upper region and large temperature difference between the inner and outer pipe walls occur until dimensionless time 8.58 during the interface level changes.
2. At dimensionless time 28.5, the maximum dimensionless temperature difference is about 0.83 between the upper and lower section of inner pipe wall surface. The temperature difference of inner wall has somewhat greater than that of outer wall. At the time, the maximum thermal stress by thermal stratification is calculated about 322 MPa in the inner wall.
3. At dimensionless time 7.5, the maximum mean Nusselt number is obtained. After this time, $\overline{Nu}$ is rapidly decreases by thermal mixing between the two fluids.

Nomenclature

a : thickness ratio of pipe
B : buoyancy term in the turbulence model
Bi : Biot number
C_1, C_2, C_3, C_μ : empirical turbulence model constants
C_p : specific heat
D_1 D_2 : diffusion coefficients
E : Young's modulus
f_1, f_1, f_μ : damping functions in the turbulence model
G : production of Turbulent kinetic energy by shear

g : acceleration of gravity
Gr : Grashof number
h : heat transfer coefficient
K : dimensionless turbulent kinetic energy
k : thermal conductivity
$\dot{m}$: mass flow rate
n : coordinate in the normal direction from the wall
Nu : Nusselt number
Pr : Prandtl number
r : dimensionless radius
Re : Reynolds number
Re_n, Re_t : local Reynolds number
Ri : Richardson number
P : dimensionless pressure
P^* : thermohydraulic pressure
T : dimensionless temperature
S : source term
t : dimensionless time
u, v : dimensionless velocities in the θ and r directions
α : thermal diffusivity
β : coefficient of thermal expansion
Γ : exchange Coefficient
Θ : angle between the top (or bottom) and interface
θ : angle
ε : dimensionless dissipation rate of turbulent kinetic energy
μ : molecular viscosity
μ_t : dimensionless turbulent viscosity
ν : kinetic viscosity
σ_K, σ_K, σ_ε : turbulent Prandtl number for K, t and ε
ϕ : general dependent variable
σ : thermal stress

Subscripts

b, m : bending and membrane
f, s : fluid and solid regions
HL : Hot Leg
hot, *cold* : hot and cold regions
i, o : inside and outside
Pzr : Pressurizer
atm : atmosphere

Superscripts

m : iteration number
$*$: physical quantity
$-$: mean value

References

1. ASME B 31.1 and Sec. II, Edition (1992)
2. ASTM A376/A376M-91a.
3. Davidson. L., "Calculation of the Turbulent Buoyancy-Driven Flow in a Rectangular Cavity Using an Efficient Solver and Two Different Low Reynolds Number K-ε Turbulence models, "Numerical Heat Transfer, Part A, Vol. 18, pp. 129-147 (1990)
4. Dhir, V.K., Amar, R.C., and Mills, J.C., "An one dimensional model for the prediction of stratification in horizontal pipes subjected to fluid temperature transient at inlet ; Part 1 : Hydrodynamic model and Part 2 ; Thermal model", *Nuclear Engineering and Design*, Vol. 107, pp. 307~325 (1988)
5. Ensel, C., Colas, A., and Barthez, "Stress analysis of a 900 MW pressurizer surge line including stratification effect", *Nuclear Engineering and Design*, Vol. 153, pp. 197~203 (1995)
6. Farouk, B., "Laminar and Turbulent Natural convection Heat Transfer from Horizontal Cylinder, ph. D thesis, Univ. of Delaware (1981)
7. Fraikin, M.P., Portier, J.J. and Fraikin, C.T., "Application of K-ε Turbulence Model to an Enclosure Buoyance Driven Recirculation Flow". ASME paper, No. 80-HT-68, July. pp. 1-12 (1980)
8. Guyette, M., "Prediction of fluid temperatures from measurements of outside wall temperatures in pipe", *Journal of Pressure Vessel Technology*, Vol. 116, pp. 179~187 (1994)
9. Kim, J.H., Ridt, R.M and Deardorff, A.F., "Thermal stratification and reactor piping integrity", Nuclear

Engineering and Design, Vol. 139, pp. 83~95 (1993)

10. Launder, B.E. and Spalding, D.B., "The Numerical Computation of Turbulent Flows" Computer Methods in Applied Mechanics and Engineering, vol. 3, pp. 269~289 (1974)
11. NRC, "Thermal stress in piping connected to RCS", Bulletin No. 88~08 (1988)
12. NRC, "Pressurizer surge line thermal stratification, Bulletin No. 88~11 (1988)
13. Patankar, S.V., "Numerical heat transfer and fluid flow", McGraw-Hill Book Company (1980)
14. Shah, V.N., and MacDonald, P.E., "Residual life assesment of major light water reactor components-Overview Volume 1", NUREG/CR-4731 EGG-2469, Vol. 1, pp. 46~62 (1989)
15. Talja, A., and Hansjosten, E., "Result of thermal stratification test in a horizontal pipe line at the HDR-Facility", *Nuclear Engineering and Design*, Vol. 118, pp. 29~41 (1990)
16. Viollet, P.L., "Observation and numerical modelling of density currents resulting from thermal transients in a non rectilinear pipe, J. of Hydraulic Research, Vol. 25, No. 2, pp. 235~261 (1987)
17. Wolf, L.,Hafner, W.,Geiss. M, Hansjosten. E, and Katzenmeier. G, "Result of HDR-Experiments for pipe load under thermally stratified flow conditions", *Nuclear Engineering and Design*, Vol. 137, pp. 387~404 (1992)